Lawrence Berkeley National Laboratory
Recent Work

Title

Measurement of Fracture-Induced Anisotropy in Shear-Wave Attenuation and Velocity from VSP Data

Permalink

https://escholarship.org/uc/item/7p29v9v6

Author

Daley, T.M.
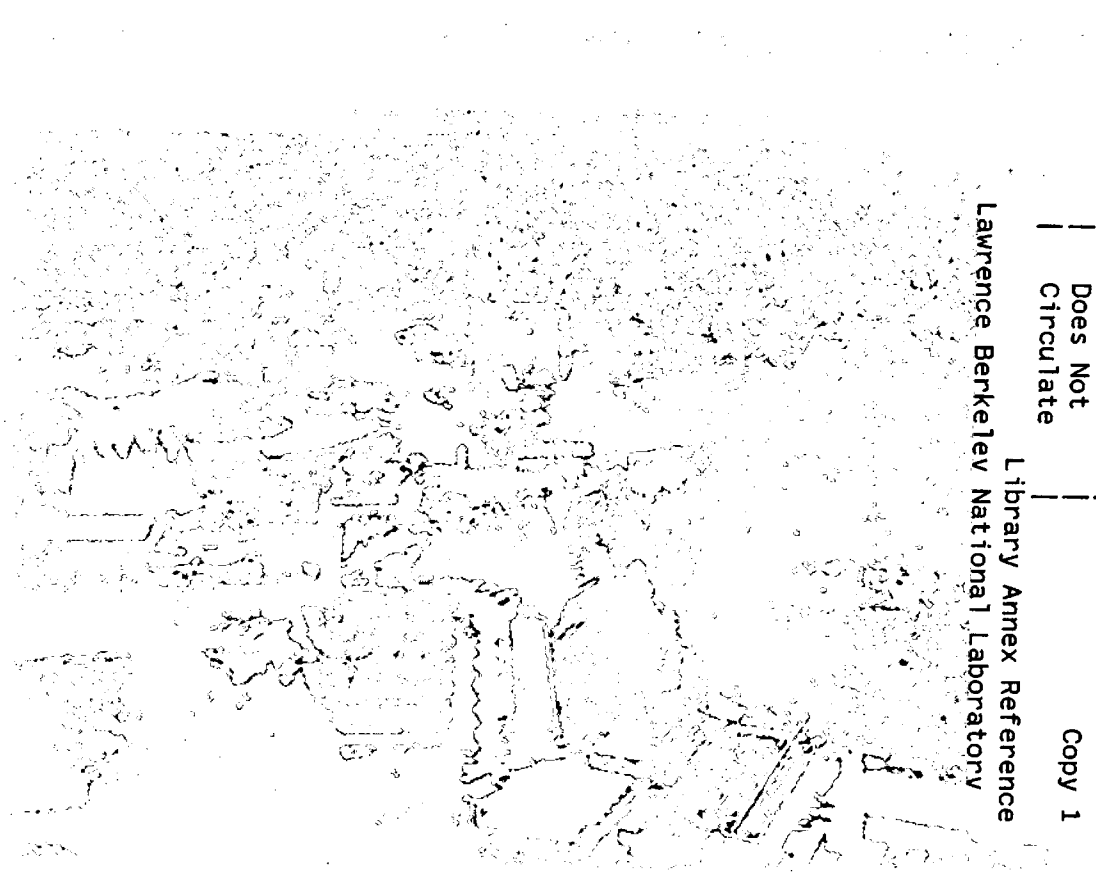
Publication Date

1996-10-01

ERNEST ORLANDO LAWRENCE BERKELEY NATIONAL LABORATORY

Measurement of Fracture-Induced Anisotropy in Shear-Wave Attenuation and Velocity From VSP Data

T.M. Daley, M. Leonard, E.L. Majer,
J.H. Queen, and V.D. Cox

Earth Sciences Division

October 1996

DISCLAIMER

Measurement of Fracture-Induced Anisotropy in Shear-Wave Attenuation and Velocity From VSP Data

T.M. Daley, M. Leonard, E.L. Majer, J.H. Queen, and V.D. Cox

Earth Sciences Division
Ernest Orlando Lawrence Berkeley National Laboratory
University of California
Berkeley, California 94720

October 1996

Measurement of Fracture-Induced Anisotropy in Shear-Wave Attenuation and Velocity From VSP Data

T. M. Daley, M. Leonard, E. L. Majer, J. H. Queen* and V. D. Cox*
Lawrence Berkeley Laboratory, Berkeley, CA
* Conoco Inc., Exploration Research and Services, Ponca City OK.

Abstract

A nine-component VSP was acquired in a 3000 ft. well at the Conoco test site in Newkirk, OK with the intent of measuring subsurface fracture properties. This site has been the subject of previous geologic and geophysical studies which have interpreted fracture properties and fracture-induced seismic anisotropy for a vertical fracture set. We use the zero-offset shear-wave VSP data, modified by a 4-component Alford rotation, to approximate a data set polarized normal and tangential to the dominant fracture orientation. This rotated data set has shear-wave polarizations aligned with the subsurface anisotropy axis of symmetry. The Alford rotation angles, determined from the shear-wave first arrivals, indicate a N67°E azimuth for the axis of symmetry. This azimuth is consistent with previous studies.

After rotation, we observe that these two shear-wave data sets have a maximum 3.3% velocity anisotropy. The observed shear-wave splitting does appear to vary with depth, implying variation in fracture properties with depth. We use the spectral ratio method to measure attenuation (Q), as a function of depth, for both polarizations. We use adaptive multi-spectral tapering to improve the spectral estimates used for the spectral ratio. We observe anisotropy in shear-wave attenuation. The tangential polarization (tangential to the fracture orientation) has a larger Q than the normal polarization (normal to fracture orientation). The average Q anisotropy is 55%.

We attempt to interpret depth-dependent changes in velocity anisotropy and Q anisotropy, however scatter in the Q values does not allow detailed interpretation. The velocity anisotropy data does allow interpreted in terms of isotropic and anisotropic regions.

Introduction

In many sedimentary formations, fractures are an important component of the sub-surface physical properties. The detection of fractures with seismic methods is an active area of research. Previous experiments using vertical seismic profiles (VSP) have shown their usefulness for understanding seismic wave propagation as a function of depth near a well. The VSP technique also has been applied to studies of wave propagation in fractured rock. In this study we have acquired and analyzed VSP data in order to obtain information about fracture properties and seismic wave propagation within a sedimentary formation. We have determined the dominant fracture orientation and measured anisotropic attenuation and velocity for shear-waves. We believe the field measurement of anisotropic S-wave attenuation is a useful extension to the study of fractured materials.

Previous researchers have used VSP measurements of shear-wave anisotropy for determination of the dominant subsurface fracture orientation (e.g.. Robertson and Corrigan, 1983, Peacock and Crampin, 1985, Majer et al, 1988, Daley et al, 1988, etc.). Recently, changes in VSP S-wave measurements have been used to detect induced fractures (Meadows and Winterstein, 1994). Unfortunately, previous studies often provided results which could not be confirmed because the local fracture properties were not well determined. Recent cooperative work between Conoco Inc. and the Lawrence Berkeley Laboratory (LBL) has provided a VSP data set acquired in a location whose fracture properties are fairly well understood. Using results from this study, we are able to show a relationship between dominant fracture orientation and shear-wave anisotropy. The symmetry axis of anisotropy determined from this VSP shear-wave data shows an unambiguous agreement with the axis of dominant fracture orientation determined from other geological and seismological studies.

In this paper, we show a measurement of shear-wave attenuation anisotropy using the spectral ratio method in conjunction with a 4-component Alford type trace rotation. Anisotropic attenuation is a wave propagation effect which is much less studied in field data than velocity or polarization. The measurement of anisotropic attenuation provides an independent seismological constraint on the cause of the anisotropy. Fracture induced anisotropic attenuation has been measured in core samples (Pyrak-Nolte, et al, 1990a) and in scale models (Ebrom, et al, 1990). Theoretical explanations of wave propagation across fractures which include anisotropic attenuation have been developed for discrete fractures (Pyrak-Nolte, et al., 1990b) and for micro-crack equivalent media (Hudson 1981, Crampin 1984). However field methods such as VSP have many inherent problems which hinder the use of attenuation measurements (White, 1992). We have improved the standard spectral ratio estimate of attenuation by using a multi-spectral tapering method for the short time windows associated with the direct shear-wave arrival. We feel the shear-wave attenuation anisotropy observed in our data set is large enough in magnitude and measured accurately enough to be useful in the determination of fracture properties.

Background and VSP Acquisition

The VSP was acquired in well 33-1 at the Conoco borehole test facility in Kay county, Oklahoma. This facility was developed for tests of well logging technology and is not a petroleum producing site. Well logging and coring of various wells at the test facility show

it to be a layered sedimentary section with natural fracturing. The characterization of subsurface geology and fracturing is well described by Queen and Rizer (1990) and the site has been reported on in numerous associated studies (e.g., Lines,et al. 1992, Lou and Crampin, 1991, Liu, et al., 1991).

Queen and Rizer (1990) describe surface geologic studies, borehole televiewer (BHTV) data, point load tests on cores, and two VSP experiments separate from the one reported on here. Their conclusions clearly indicate vertical fracturing with a regional orientation described as a "systematic component subparallel to the ENE" direction. Previous VSP studies at the Conoco site used either multiple P-wave source locations at a few depths, or a single location for P and SH sources at multiple depth intervals. The VSP experiments described by Queen and Rizer indicate an azimuth of N75°E for the anisotropy symmetry axis, although there is ambiguity in the data. This ambiguity in previously acquired VSP data is one reason for acquiring the VSP described in this paper which provides complimentary, not redundant, information.

Our VSP is 9-component, with three source types and a three component receiver. Data was recorded at 50 ft. (15 m) depth intervals (Fig. 1a). The receiver was a three-component wall-locking borehole geophone. The sources were a P-wave and two orthogonal shear-waves. The shear-wave source was Amoco's shear-wave vibrator which can switch between in-line and transverse polarizations without moving. This switching capability is important for the consistency of amplitude given to shear-waves. A P-wave vibrator was used at three separate source locations, one nearly coincident with the shear-wave source, and two on separate azimuths to provide alignment information for the geophone's horizontal components (Fig. 1b). By recording these sources every 50 ft., it was hoped to use the 9-component data to detail the effects of shear-wave anisotropy and to provide better depth sampling and resolution than previous surveys. The sweeps used were 51 to 6 Hz for shear and 102 to 12 Hz for P, both 30 seconds long with an extra 2 seconds listen time. The shear-wave source was moved twice during acquisition because the baseplate was digging into the soil. The shear-wave source offset distances were 99, 118 and 128 ft. (30, 36 and 39 m) at an azimuth of 279°; the P-wave vibrator was always 35 ft. (10) m behind the shear-wave vibrator. The other two P-wave vibrators were at offsets of 700 and 1500 ft. (213 m and 457 m) at a 155° azimuth.

Methods of Measurement and Analysis of Anisotropy

Analysis of the 9-component VSP data for well 33-1 focused on indications of seismic anisotropy as indicated by shear-wave splitting (a difference in travel-time between orthogonally polarized shear-waves). We began with stacked and edited data from each source. Because the horizontal receiver components were recorded with random orientation due to downhole tool rotation while moving between depth locations, we used the P-wave first arrival to determine the orientation. The particle motion of the P-wave was assumed to be in the source-receiver vertical plane. We determined the orientation of the P-wave particle motion using the eigenvectors of the data covariance matrix (Kanasewich, 1981). The horizontal geophone data was then numerically rotated into in-line and cross-line orientations (with respect to a line connecting source and receiver). This provided a data set with vertical, horizontal-radial and horizontal-transverse receiver components for each source. This 9-component data set is shown in Fig. 2.

Initial interpretation of the data for shear-wave anisotropy can be made using the travel-time difference between arrivals for the SV-source radial-receiver data and the SH-source transverse-receiver data. Travel-time differences provide a depth dependent measure of the shear-wave splitting caused by anisotropic propagation. However these travel times only give a magnitude of anisotropic effects for the particular azimuthal orientation of the source-receiver pair. The analysis of shear-wave VSP data for transversely isotropic media with a vertical axis of symmetry can be improved by the application of a 4-component rotation technique. This rotation, often termed an Alford rotation (Alford ,1986), gives the angles at each recording depth which best decompose the four seismic traces into two traces. These are the two traces which best represent data recorded in the natural polarization direction of a transversely isotropic media. For vertically propagating, orthogonally polarized shear-waves, the 4-component rotation can give an azimuthal orientation of the axis of symmetry of anisotropy (and by implication, the orientation axis of natural fractures). This method of 4-component rotation, originally proposed by Alford (1986), with further development by Thomsen (1988), was recently demonstrated in field experiments by Winterstein and Meadows (1991). Thomsen shows that for a set of orthogonal shear-wave sources and receivers, which are oriented at an angle θ to the symmetry azimuth of anisotropy, we can determine θ and construct the "principal time series". These are the time series which would be recorded if the sources and receivers were oriented along θ. Queen and Rizer (1990) nicely describe this operation in terms of a band-limited tensor transfer function between acquisition coordinates and symmetry coordinates. Winterstein and Meadows apply this 4-component rotation method and extend it by proposing a layer stripping scheme which allows more accurate measurement of anisotropy azimuth at depth and measurement of changes in θ as a function of depth. We further apply the 4-component shear-wave rotation to measurement of shear-wave attenuation anisotropy in the symmetry coordinate system.

Figure 3 shows the calculated 4-component rotation angles. These angles are computed from the azimuth of the in-line shear-wave source and then corrected for that azimuth to give an angle from North. The average angle is 67° with a standard deviation of 4.1°. However, please note that the true accuracy is affected by the original geophone rotation based on P-wave polarization which has accuracy on the order of 10°. The 67° angle agrees well with the previously inferred fracture orientation (Queen and Rizer, 1990), and the angles show remarkable consistency as a function of depth. We feel this result is accurately portraying the dominant fracture orientation as a function of depth. Note that the S-wave splitting is clearly measurable at the shallowest receiver depth of 500 feet. This agrees with other studies at the Conoco test facility which show fracturing in shallow formations such as the Ft. Reilly limestone (Queen and Rizer, 1990).

Figure 4 shows the two component data which are the diagonal of the 4-component tensor rotation. This is the data which best corresponds to alignment with the subsurface's anisotropy axis of symmetry. The data in Fig. 4 is now in-line (tangential) with and cross-line (normal) to the axis of symmetry, not the source-receiver line. The in-line data is polarized parallel to the dominant fracture azimuth and the cross-line data is polarized perpendicular to the dominant fracture azimuth.

Figure 5 shows the travel-time difference using the in-line and cross-line traces from Fig. 4. Travel times were obtained by picking the first major amplitude peak for each data trace. The travel-time difference is increased from the original recordings (Fig. 2) because the 4-component rotation gives the data a new coordinate system (the anisotropy coordinate system) which maximizes travel-time splitting for an azimuthally anisotropic system.

The maximum travel-time difference of about 0.02 s in a total travel time of 0.6 s is 3.3% average anisotropy in shear-wave velocity.

Inspection of the travel time difference data suggests three types of depth zones. These zones are as follows:

1) Zones of consistently increasing time difference, e.g. 500 to 700 ft., 1000 to 1150 ft., 1650 to 2250 ft.

2) Zones of no increase in time difference, e.g. 1350 to 1650 ft., 2600 to 2950 ft. (except 2850).

3) Zones of inconsistent time differences, e.g. 800 to 1000 ft., 2250 to 2500 ft.

These can be interpreted as regions of isotropy, anisotropy and transitional or interference regions, respectively. In an anisotropic zone, the split shear-waves will continue to separate in time as the waves propagate. In an isotropic zone, the split shear-waves will maintain their time difference. In zones where the anisotropy axis is changing, or where other converted waves interfere with the direct arrivals (such as at reflecting horizons) changes in the split shear-wave wavelets will give scattered time differences. Because the rotation angles are consistent with depth, we do not feel the zones of inconsistent time difference are due to changes in the anisotropy axis of symmetry. A more probable cause is S-wave reflections or S to P conversions.

The measurement of attenuation anisotropy begins with the in-line and cross-line components of the 4-component rotated data shown in Fig 4. In addition to maximizing the observable travel-time anisotropy, the Alford rotation also has the potential for maximizing anisotropic attenuation effects in the data. Theoretically, we would expect the cross-line wavefield to experience greater attenuation due to theoretical predictions made by Crampin (1984) for the micro-crack model. Pyrak-Nolte, et al (1990a) have a singularity in their discrete fracture model for the geometry of our acquisition, so prediction is not possible..

Our attenuation estimates are obtained using the method of spectral ratios. Essentially, in this method one computes the ratio of amplitude spectra between two down-hole recordings and fits a straight-line slope to this ratio versus frequency. The inverse value of this slope scaled by the difference in travel time yields an estimate of the net attenuation, Q, between the recordings. The estimation of Q in this manner from borehole data and the difficulties involved are discussed by Sams and Goldberg (1990), among others. One difficulty is the contamination of spectral ratios due to time-domain windowing effects. To combat this problem we compute spectral ratios using the adaptive multitaper spectral estimation method, described by Thomson (1982) and Park et al. (1987). The advantage of the multitaper method over standard windowing techniques is its ability to greatly reduce spectral leakage and produce relatively low bias, low variance estimates. For our spectral estimates we use the first seven 4π multitapers. To reduce spectral leakage even further the windowed data are pre-whitened prior to applying the tapers.

The spectral time window is centered on the direct S-wave arrival and spans 0.25 seconds. The spectra are calculated at each depth for both in-line and cross-line components of the Alford rotation. Figure 6 displays representative spectra for each component. The spectral ratios for each depth are then calculated using a shallow recording (550 feet) as a reference. The slopes of these ratios yield the net attenuation between the 550 feet reference depth and the depth to each recording. Unweighted least squares fits to the ratios are done between 10 Hz and 50 Hz, beyond which is an excessively low signal to noise ratio. The resulting net Q values are shown in Figure 7 for both the in-line and cross-line data sets.

For both in-line and cross-line data sets we see that the net attenuation tends to increase with depth, as would be expected due to increased ground compaction. We also see a difference in Q between the in-line and cross-line data. This observation is our measurement of S-wave attenuation anisotropy in the fractured subsurface. As theoretically predicted (Crampin 1984) for a system of aligned micro-cracks, the cross-line data show consistently lower Q (greater attenuation) than the in-line data. We have not attempted to interpret the Q anisotropy in terms of micro-crack density or aperture because geologic studies of the area clearly indicate discrete large scale fracturing. The fracture stiffness theory developed by Pyrak-Nolte, et al (1990a) has an amplitude singularity for our geometry (vertical fractures and vertically propagating shear-waves). Therefor we do not have an adequate theoretical basis for interpreting our shear-wave attenuation anisotropy in terms of geologically realistic fracture properties.

We observe in Fig. 7 that the in-line Q values have more scatter than the cross-line Q values. We also observed that the in-line data set had larger standard deviation for the fit of spectral ratio slope. We can quantify this apparent difference in accuracy by fitting each set of Q values to a line and calculating the standard deviation for each line. The in-line data set (which was interpolated for three Q values greater than 300) has a standard deviation of 35.1, while the cross-line standard deviation is 8.5.

The Q anisotropy at 2900 ft. (defined as $(Q_i - Q_x)/Q_i*100$) is 36% and the mean Q anisotropy for all depths is 55.2% with a standard deviation of 19.4. While scatter and uncertainty in the Q estimates (particularly for the in-line data) degrade our ability to interpret the variations in Q, the attenuation anisotropy does appear to change with depth. Fig. 8 shows the Q difference as a function of depth with a polynomial fit. From 600 to about 1250 ft., the Q difference is increasing, from 1250 ft. to about 2500 ft. the Q difference is relatively constant (implying more isotropic propagation) and below 2500 ft. Q difference appears to increase again. Note that the scatter in Q values makes depth dependent interpretation of Q more difficult than interpretation of velocity anisotropy.

While it is tempting to interpret the depth dependent Q anisotropy variations as changes in fracture density, aperture or stiffness, we are most comfortable with the basic observation and measurement of attenuation anisotropy in shear-wave VSP data.

Conclusions

We have directly measured fracture-induced shear-wave attenuation anisotropy in VSP data. We believe the combination of multi-component rotation and multi-spectral tapering for spectral ratios gives good resolution of this depth dependent amplitude anisotropic effect for the bandwidth of our VSP data. The shear waves polarized tangential to the fracturing have a net Q nearly twice that of the shear waves polarized normal to fracturing. We feel the 55% average Q anisotropy is significant enough to overcome any misgivings about the accuracy of amplitude measurements from VSP. The anisotropic nature of the Conoco test site has been documented by previous work, and the shear-wave splitting (velocity anisotropy) observed in this study confirms the previous studies. We measure a shear wave velocity anisotropy of about 3.3%. We have inferred the orientation of the anisotropy axis of symmetry via the rotation angles of the 4-component rotation. These angles show a consistent orientation of N67°E. This azimuth is consistent with previous studies of fracture orientation at this site.

The measurement of shear-wave Q anisotropy in addition to velocity anisotropy

should allow further constraints to be placed on in-situ fracture properties. We do observe a variation in Q anisotropy with depth which potentially could be used to interpret variations in fracture properties within this formation. However, we are not able to find a theoretical prediction of fracture-induced shear-wave attenuation anisotropy for the large scale discrete fractures believed to exist at this site.

THE END

References

Alford, R.M., 1986. Shear data in the presence of azimuthal anisotropy, 56th Ann. Internat. Mtg., Soc. Explor. Geophys., Expanded Abstracts, 476-479.

Crampin, S., 1984. Effective anisotropic elastic constants for wave propagation through cracked solids, Geophys. J. R. astr. Soc., 76, 135-145.

Daley, T.M., T.V. McEvilly, and E.L. Majer, 1988. Analysis of P and S Wave Vertical Seismic Profile Data From the Salton Sea Scientific Drilling Project, J. Geophys. Res., 93, B11, 13025-13036.

Hudson, J.A., 1981. Wave speeds and attenuation of elastic waves in material containing cracks, Geophys. J. R. astr. Soc., 64, 133-150.

Kanasewich, E. R., 1983. Time Sequence Analysis in Geophysics. The University of Alberta Press, p336.

Majer, E.L., T.V. McEvilly, F. Eastwood, and L. Myer, 1988. Fracture detection using P- and S-Wave VSPs at The Geysers geothermal field, Geophysics, 53, 76-84.

Park, J., C. R. Linberg, and F. L. Vernon III, 1987. Multitaper spectral analysis of high-frequency seismograms, J. Geophys. Res., 92, 12675-12684.

Peacock S., and Crampin S., 1985, Shear-wave vibrator signals in transversely isotropic shale, *Geophysics, v50*, n8, p1285-1293.

Pyrak-Nolte, L. J., Myer, L. R., Cook, N. G., 1990b. Transmission of Seismic Waves Across Single Natural Fractures, Journal of Geophysical Res., 95, 8617-8638.

Pyrak-Nolte, L. J. Myer, L.R., Cook, N.G., 1990a. Anisotropy in Seismic Velocities and Amplitudes from Multiple Parallel Fractures, Journal of Geophysical Research, Vol. 95, B7, 11345-11358.

Queen, J. H. and Rizer, W. D., 1990. An Integrated Study of Seismic Anisotropy and the Natural Fracture System at the Conoco Borehole Test Facility, Kay County, Oklahoma, Jou. of Geophysical Res., v. 95 p. 11255-11273.

Robertson, J.D., and D. Corrigan, 1983, Radiation patterns of a shear-wave vibrator in near-surface shale, Geophysics, 48, 1,19-26.

Sams, M. and D. Goldberg, 1990. The validity of Q estimates from borehole data using spectral ratios, Geophysics, 55, 97-101.

Thomsen, D. J., 1982. Spectrum estimation and harmonic analysis, IEEE Proc., 70, 1055-1096.

Thomsen, L., 1988. Reflection seismology over azimuthally anisotropic media, Geophysics, 53, 304-313.

White, R. E., 1992. The accuracy of estimating Q from seismic data, Geophysics, 57, 1508-1511.

Winterstein, D.F., and Meadows, M.A., 1991. Shear-wave polarizations and subsurface stress directions

at Lost Hills field, Geophysics, 56, 1331-1348.

Winterstein, D.F., and Meadows, M.A., 1994. Seismic detection of a hydraulic fracture from shear-wave VSP data at Lost Hills Field, California, Geophysics, 59, 1, 11-26.
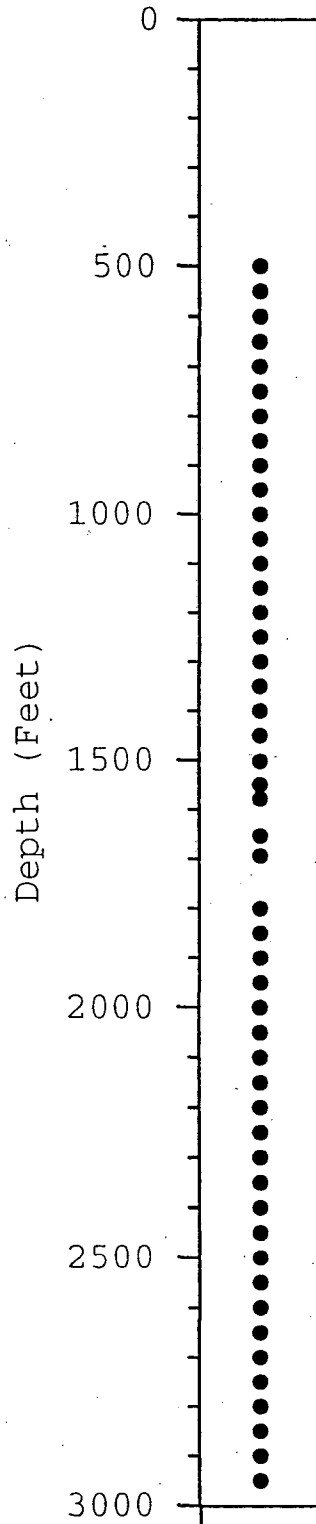
Figure Captions

Fig 1a Location of 3-component wall-locking geophone for VSP data used in this paper. The geophone spacing was 50 ft. (15 m), except where borehole washouts prevented locking (notable near 1700 ft.).
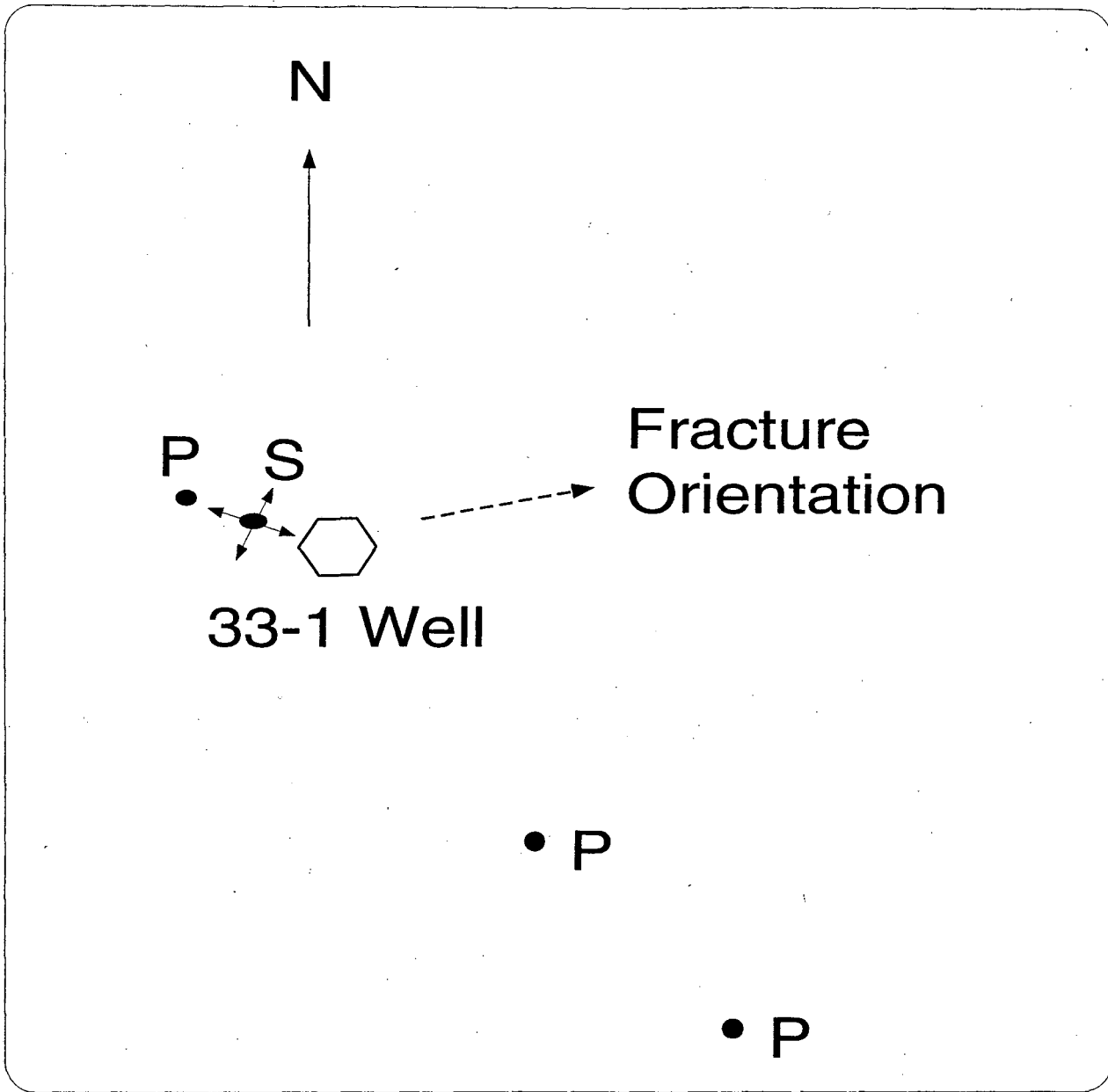
Fig 1b Approximate locations (solid dots) and polarizations (arrow heads) of VSP sources relative to well 33-1. The dominant azimuth of vertical fracturing previously determined (Queen and Rizer, 1990) is shown with dashed arrow. The two P-wave sources to the south-east were only used in this study for geophone orientaion.

Fig 1c (Left) Orientation of S-wave sources and horizontal-component sensors after initial acquisition rotation. Both source and sensors are oriented with respect to source location azimuth. Transverse source is called SH, and radial source is called SV, in text. Data in Fig. 2 uses this orientation.

 (Right) Orientation of S-wave data after 4-component (Alford) rotation. The orientation is determined by maximizing shear-wave energy on two components, thereby (by inference) orienting the S-wave polarizations with respect to dominant fracture orientation.

Fig 2. Nine-component VSP data display from near offset P- and S-wave sources. Each panel has all recorded data traces for a single sensor orientation for a single source polarization. The sensor orientations have been rotated based on P-wave polarizations from three different P-wave sources. The columns are (left to right) P-wave, S-wave radial to well (SV) and S-wave transverse to well (SH). The rows are (top to bottom) vertical component, horizontal-radial component and horizontal-transverse component. All traces are normalized to the same constant. The timing lines are spaced every 100 ms. Viewing the data panels as a (3x3) matrix (row x column), an isotropic media would have no energy on elements (3,1), (3,2), (1,3) and (2,3). The energy seen on these elements is obvious evidence of anisotropy.

Fig 3. Calculated angles for 4-component (Alford) rotation. This angle corresponds to the dominant fracture azimuth. The average angle of N67°E is slightly less than the previously inferred fracture orientation at this site (75° East of North).

Fig. 4. The rotated in-line and cross-line data resulting from 4-component rotation. The first arrivals of these traces were used for travel time and attenuation calculations. Each trace is normalized to its own peak amplitude. The travel times for Fig.5 were picked from the peak amplitude for each trace. The attenuation analysis was performed on a 250 ms window centered on the first arrival.

Fig 5. Shear-wave travel-time difference between in-line and cross-line data after 4-component (Alford) rotation (data traces shown in Fig 4). The variations in travel-time difference are used for interpretation of variations in subsurface anisotropy magnitude.

Figs 6a and 6b. Fourier amplitudes for the first arrival wavelet for two depths of the in-line (6a) and cross-line (6b) data from Fig. 5. The two spectra shown are for recording depths 550 ft. (open box marker) and 2900 ft. (solid circle marker). The 550 ft. spectra are the reference used for spectral ratio calculations. Note that only 13 spectral data points are in the bandwidth of interest (8 to 60 Hz.). The lack of shear-wave bandwidth is a limiting factor in attenuation estimates. The spectra were calculated from a 250 ms window centered on the shear-wave arrival using an adaptive multi-spectral tapering method.

Fig 7. Seismic Q for the in-line and cross-line data sets. The cross-line Q (Qi, box marker) is an average 55% of the in-line Q (Qx, dot marker). This difference in Q is the amplitude anisotropy. The Q values were calculated using spectral ratios with the 550 ft. spectrum (Fig 6) as a reference. This Q value is an interval Q from 550 ft. to each marked depth.

Fig 8. Shear-wave Q difference (Qi - Qx) is shown with dotted line and plus marks. A best fit polynomial curve is also shown (solid line). We observe an increase in Q difference from 600 to 1250 ft., a relatively stable Q difference from 1250 to 2500 ft., and a small increase below 2500 ft.

Source and Sensor Locations

Fig 1a Location of 3-component wall-locking geophone for VSP data used in this paper. The geophone spacing was 50 ft. (15 m), except where borehole washouts prevented locking (notable near 1700 ft.).

Fig 1b Approximate locations (solid dots) and polarizations (arrow heads) of VSP sources relative to well 33-1. The dominant azimuth of vertical fracturing previously determined (Queen and Rizer, 1990) is shown with dashed arrow. The two P-wave sources to the south-east were only used in this study for geophone orientaion.
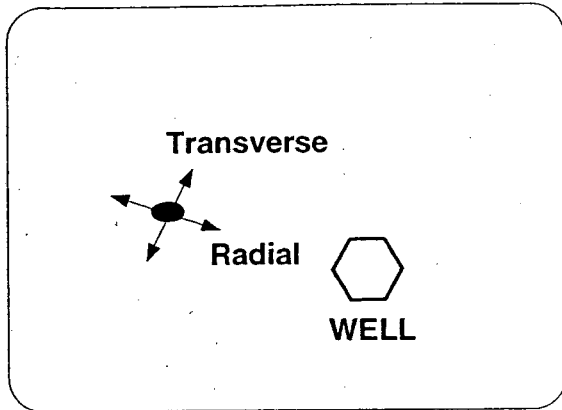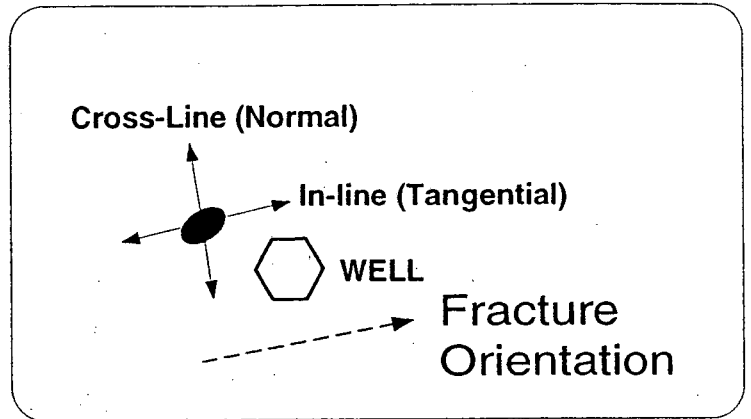
Initial Acquisition Rotation   **4 - Component (Alford) Rotation**

Fig 1c (Left) Orientation of S-wave sources and horizontal-component sensors after initial acquisition rotation. Both source and sensors are oriented with respect to source location azimuth. Transverse source is called SH, and radial source is called SV, in text. Data in Fig. 2 uses this orientation.

(Right) Orientation of S-wave data after 4-component (Alford) rotation. The orientation is determined by maximizing shear-wave energy on two components, thereby (by inference) orienting the S-wave polarizations with respect to dominant fracture orientation.

Fig 2. Nine-component VSP data display from near offset P- and S-wave sources. Each panel has all recorded data traces for a single sensor orientation for a single source polarization. The sensor orientations have been rotated based on P-wave polarizations from three different P-wave sources. The columns are (left to right) P-wave, S-wave radial to well (SV) and S-wave transverse to well (SH). The rows are (top to bottom) vertical component, horizontal-radial component and horizontal-transverse component. All traces are normalized to the same constant. The timing lines are spaced every 100 ms. Viewing the data panels as a (3x3) matrix (row x column), an isotropic media would have no energy on elements (3,1), (3,2), (1,3) and (2,3). The energy seen on these elements is obvious evidence of anisotropy.

Fig 3. Calculated angles for 4-component (Alford) rotation. This angle corresponds to the dominant fracture azimuth. The average angle of N67°E is slightly less than the previously inferred fracture orientation at this site (75° East of North).
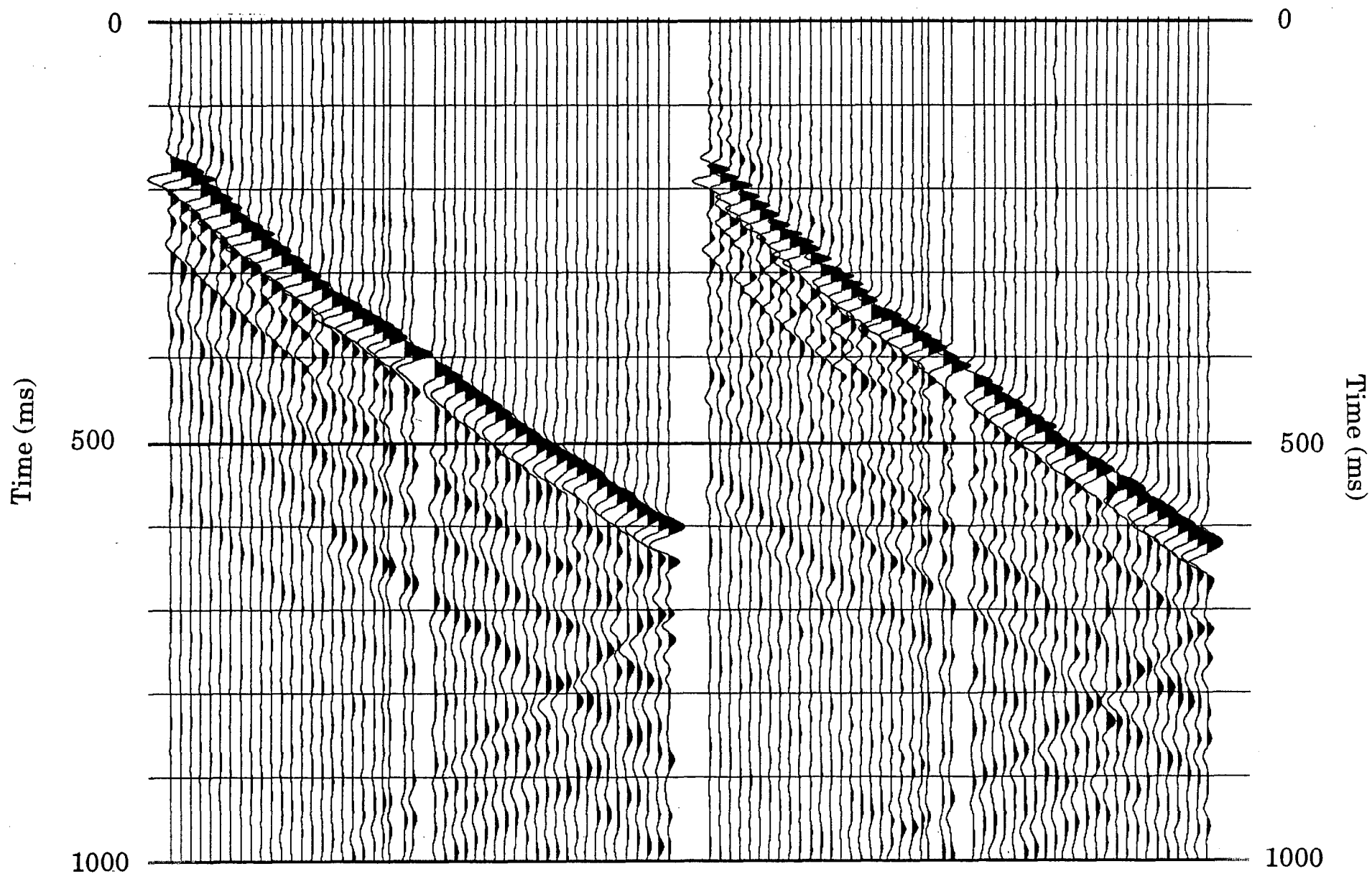
Fig. 4. The rotated in-line and cross-line data resulting from 4-component rotation. The first arrivals of these traces were used for travel time and attenuation calculations. Each trace is normalized to its own peak amplitude. The travel times for Fig.5 were picked from the peak amplitude for each trace. The attenuation analysis was performed on a 250 ms window centered on the first arrival.
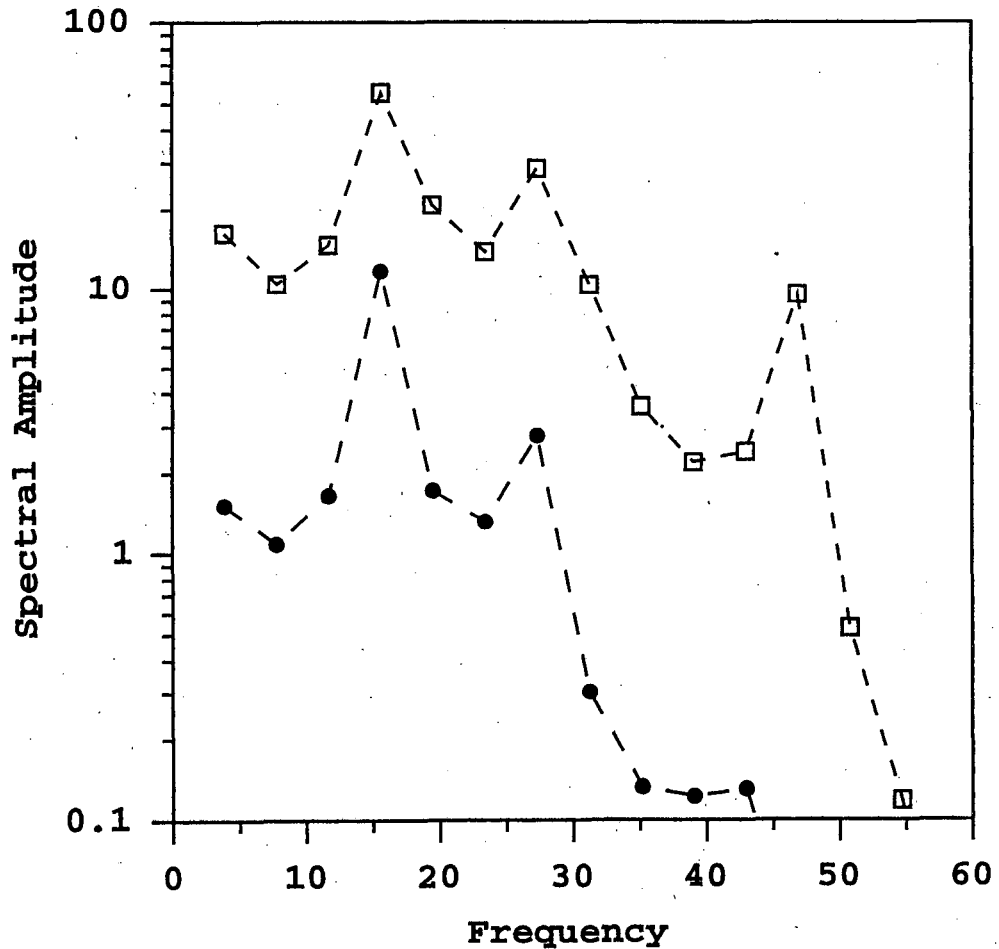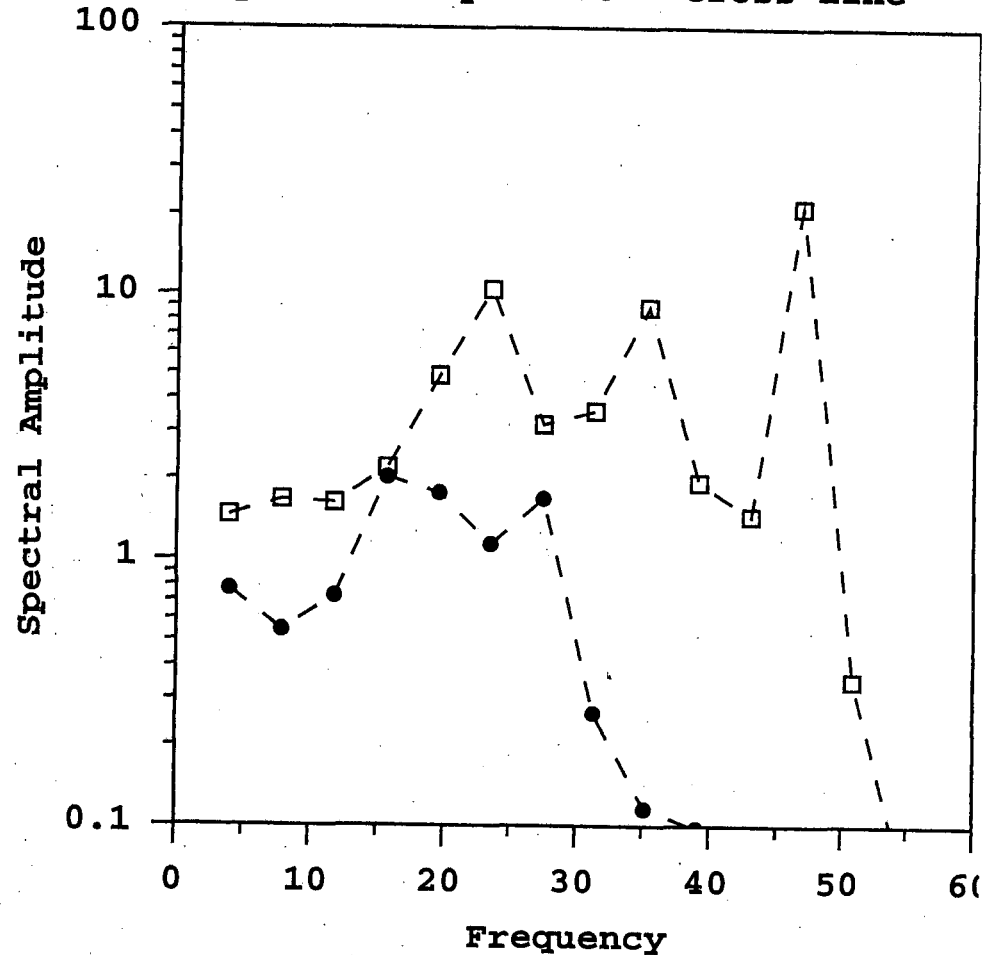
Fig 5. Shear-wave travel-time difference between in-line and cross-line data after 4-component (Alford) rotation (data traces shown in Fig 4). The variations in travel-time difference are used for interpretation of variations in subsurface anisotropy magnitude.

Figs 6a and 6b. Fourier amplitudes for the first arrival wavelet for two depths of the in-line (6a) and cross-line (6b) data from Fig. 5. The two spectra shown are for recording depths 550 ft. (open box marker) and 2900 ft. (solid circle marker). The 550 ft. spectra are the reference used for spectral ratio calculations. Note that only 13 spectral data points are in the bandwidth of interest (8 to 60 Hz.). The lack of shear-wave bandwidth is a limiting factor in attenuation estimates. The spectra were calculated from a 250 ms window centered on the shear-wave arrival using an adaptive multi-spectral tapering method.

S-Wave Attenuation Anisotropy from VSP
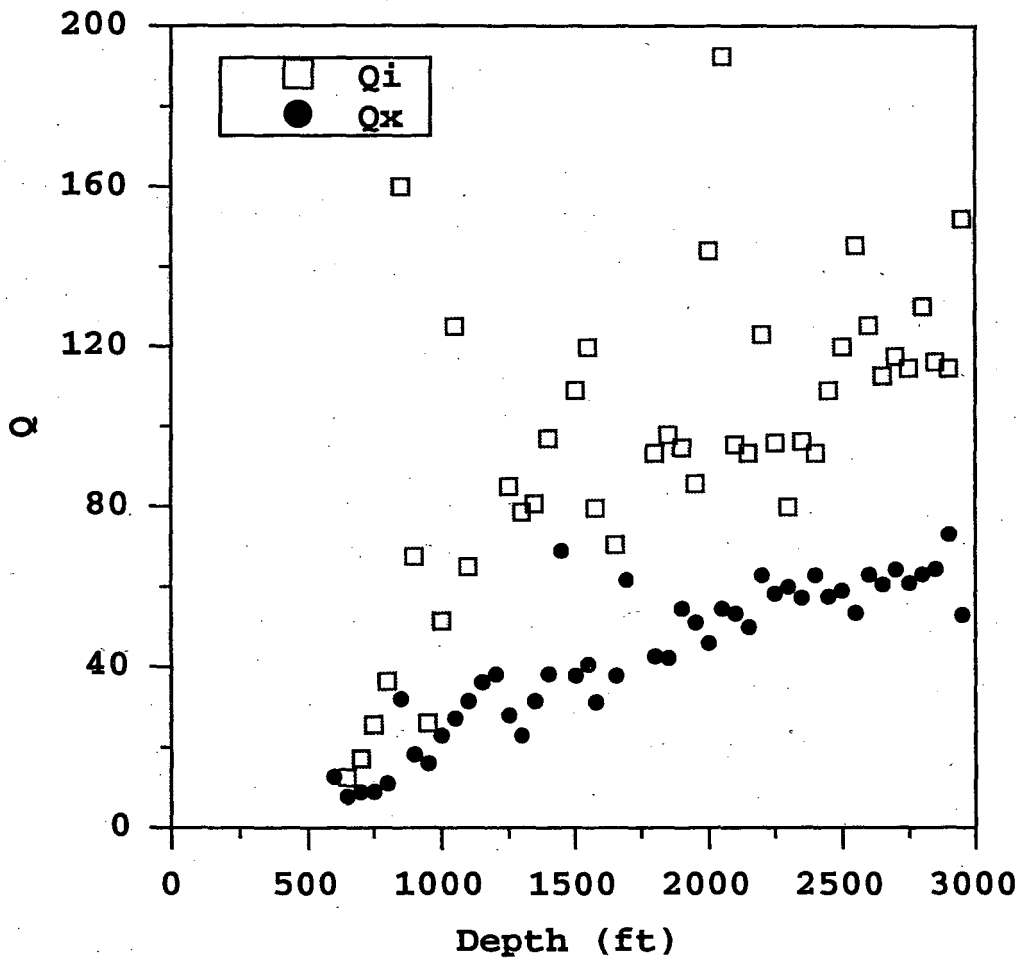## Normal (Qx) and Tangential (Qi) to Fractures

Fig 7. Seismic Q for the in-line and cross-line data sets. The cross-line Q (Qi, box marker) is an average 55% of the in-line Q (Qx, dot marker). This difference in Q is the amplitude anisotropy. The Q values were calculated using spectral ratios with the 550 ft. spectrum (Fig 6) as a reference. This Q value is an interval Q from 550 ft. to each marked depth.
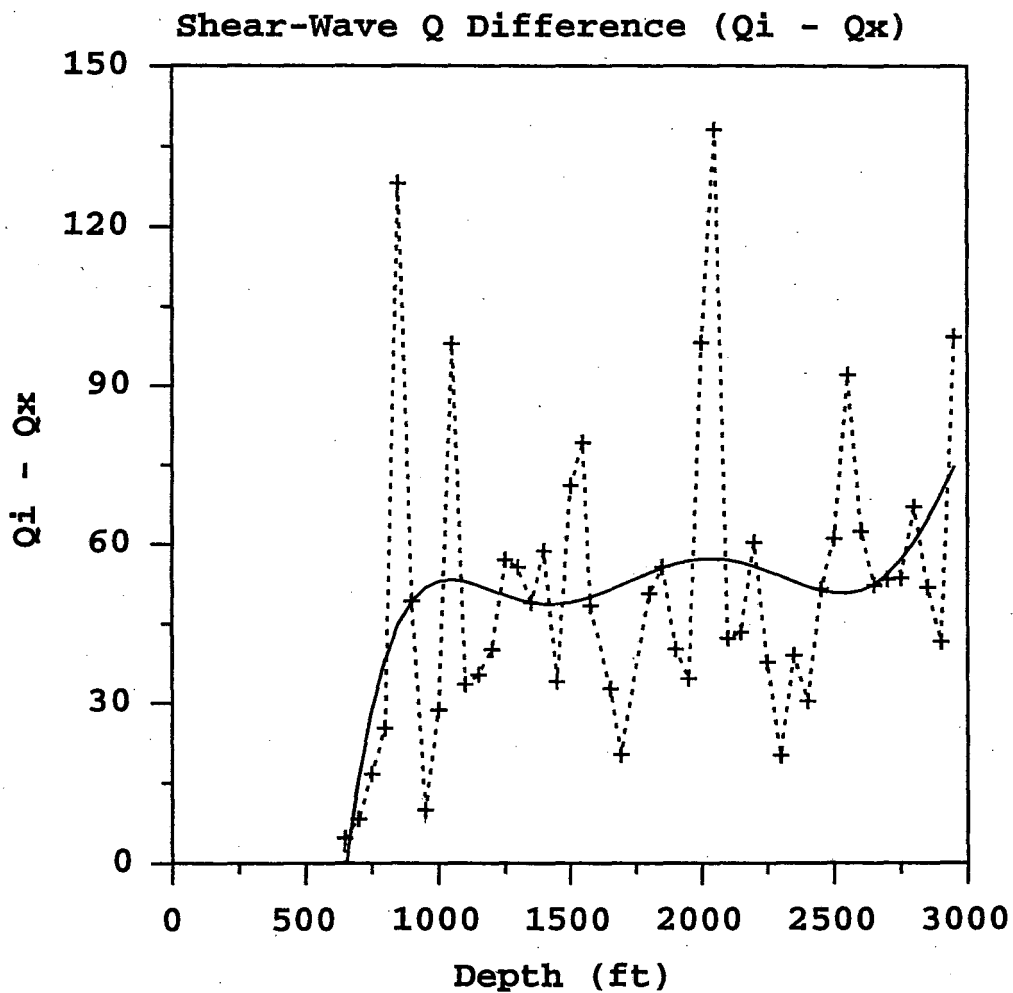
Fig 8. Shear-wave Q difference (Qi - Qx) is shown with dotted line and plus marks. A best fit polynomial curve is also shown (solid line). We observe an increase in Q difference from 600 to 1250 ft., a relatively stable Q difference from 1250 to 2500 ft., and a small increase below 2500 ft.